Journal of
Plankton Research

plankt.oxfordjournals.org

J. Plankton Res. (2014) 36(4): 1124–1134. First published online May 9, 2014 doi:10.1093/plankt/fbu031

Internal wave–zooplankton interactions in the Alboran Sea (W-Mediterranean)

HANS VAN HAREN*
ROYAL NETHERLANDS INSTITUTE FOR SEA RESEARCH (NIOZ), PO BOX 59, 1790 AB DEN BURG, THE NETHERLANDS

*CORRESPONDING AUTHOR: hans.van.haren@nioz.nl

Received January 15, 2014; accepted March 31, 2014

Corresponding editor: Roger Harris

An upward looking 75 kHz ADCP (Acoustic Doppler Current Profiler) was moored at 100 m above the bottom in 912 m water depth in the central-north Alboran Sea (W-Mediterranean Sea). The ADCP sampled current and acoustic echo-amplitude at a rate of once per minute for 9 days, thereby revealing particular internal wave–zooplankton interactions that varied with depth. The ADCP's echo-amplitude, a measure of zooplankton abundance, showed a dominant diurnal periodicity due to vertical migration, and occasionally intense reflections manifesting high-frequency interfacial internal waves close to the buoyancy frequency. These waves reached excursions of up to about 90 m crest-trough, around 250 m. They were only visible in acoustic data during daytime when the zooplankton gathered near these thin interfacial layers. Around 500 m where the vertical density stratification was 10 times smaller than at 250 m, larger amplitude internal waves were observed, measuring up to about 150 m crest-trough. These waves had the lowest internal wave frequency, close to the inertial frequency. Below 600 m, the stratification was so weak that large (∼100 m) vertical convection in the direction of the earth rotational vector dominated over internal gravity waves. At these depths, diurnal vertical migrations were not observed, which suggests that zooplankton either avoid or become dispersed by waters with large vertical convection. Light limitation is not expected to be a key factor in this case, as vertical migration has been observed deeper than 1000 m in other areas where stratification is greater.

KEYWORDS: acoustic Doppler current profiler observations; zooplankton; internal waves; biophysical interaction; variable stratification

INTRODUCTION

In aquatic environments like oceans, seas and lakes, plankton-biological and physical dynamics are often coupled (see a recent review by Prairie *et al.*, 2012). One of the fundamental physical properties of large water bodies affecting plankton dynamics is the stable vertical density stratification, by freshwater outflow in the ocean and, more generally, by solar heating from above. The stratification allows approximately neutrally buoyant phytoplankton species to stay in the less dense and light-abundant near-surface waters, for optimal growth. However, upon depletion of nutrients, less optimal conditions may apply, causing plankton to reside in deeper waters. Such a scenario can apply for the open ocean (Sverdrup, 1953), but not necessarily for turbulent shallow seas (van Haren *et al.*, 1998).

The spatial variation in density results in several important effects on phytoplankton distribution (e.g. McManus *et al.*, 2003), (i) horizontal gradients or fronts bordering different water masses are known plankton accumulation regions due to a varying nutrient supply, (ii) thin horizontal layers spread material along isopycnals from lateral boundaries and may hamper vertical exchange so that nutrient-rich and poor waters are separated vertically, (iii) internal (interfacial) waves move such thin layers up and down by up to 100 m crest-trough, thereby moving the collected plankton in and out of the photic zone, (iv) nonlinear internal waves may break and cause diapycnal turbulent mixing for redistribution of materials. On the other hand, large amounts of plankton may (weakly) influence the stratification, and thereby the physics of the environment.

Although the vertical density stratification is generally statically stable, it may support considerable de-stabilizing vertical current differences 'shear' to the point of marginal (dynamic) stability (van Haren *et al.*, 1999). This shear is predominantly near the inertial frequency f, the lowest internal wave frequency in stratified waters. This is because the vertical length-scale of near-inertial waves is small (LeBlond and Mysak, 1978). The shear may interact with fronts to transfer vertical isopycnals to the horizontal, to create thin layers and associated phytoplankton accumulating density interfaces (Franks, 1995). Dekshenieks *et al.* (Dekshenieks *et al.*, 2001) estimated that 40–50% of these thin layers have a thickness of <1 m and 80% <2 m. The phytoplankton may support an enhanced stock of zooplankton or other predators at the interface (McManus *et al.*, 2003).

The vertical extent of the shear relative to the interface thickness may have two effects on its environment. First, it determines the amplitude of interfacial internal waves before breaking (Linden, 1979). Besides varying the layer thickness through straining, these high-frequency internal waves near the buoyancy frequency locally add shear to the 'background' inertial shear. Second, it may collect daily vertically migrating (DVM) phytoplankton at depths where the shear exceeds a certain threshold value so that these plankton tumble and loose orientation, 'gyrotactic trapping' as one of the means to enhance (phyto)plankton at an interface, see the overview by Durham and Stocker (Durham and Stocker, 2012).

Thus far, most research on biophysical interactions has focused on near-surface waters (<50 m) and phytoplankton (e.g. Lennert-Cody and Franks, 1999; McManus *et al.*, 2003; Huber *et al.*, 2011). Less attention has been given to zooplankton, which have more active swimming capabilities, and to deeper waters (>100 m). Deep (>500 m) convective areas have not often been studied in connection with plankton species, an exception being Stemmann *et al.* (Stemmann *et al.*, 2008), who however focused on the effects of frontal advection.

In the present article, moored acoustic observations are investigated between about 200 and 800 m. All are well below the euphotic zone, and the 75 kHz transmit frequency of the acoustic device ensures predominant reflection off zooplankton of sizes >0.01 m (Frassetto *et al.*, 1961; RDI, 1996) because the waters are not highly turbulent (Warren *et al.*, 2003). As the observations were made over a vertical range over which stratification varied from strong to weak (near-homogeneous), three parameters associated with biophysical interactions could be studied: high-frequency interfacial internal waves, low-frequency internal wave induced turbulent convection and zooplankton DVM. In contrast with the effects of phytoplankton, stratification itself unlikely affects zooplankton DVM. The variations in buoyancy are small and do not seem to hamper DVM, as all are observed in well-stratified waters (e.g. Frassetto *et al.*, 1961; Plueddemann and Pinkel, 1989; van Haren, 2007). However, shear associated with stratification can affect vertical migration, by variable horizontal dispersal of plankton. This may not be noticeable in acoustic observations, when the zooplankton migrate over large areas and individuals are not registered in echoes, only ensembles. Likewise, the stratification can support (high frequency) internal waves, with vertical speeds comparable with those of the plankton. As such waves have much shorter periodicities (of typically half-an-hour duration), the effects on zooplankton DVM will average out during the 2–3 h ascent and descent.

The observations were made during monitoring the environmental conditions as a support for multiple test series of experimental mooring-deployment devices for the future cubic kilometre neutrino telescope (KM3NeT; http://www.km3net.org/home.php). The test site was in the central-north Alboran Sea, West Mediterranean (Fig. 1).

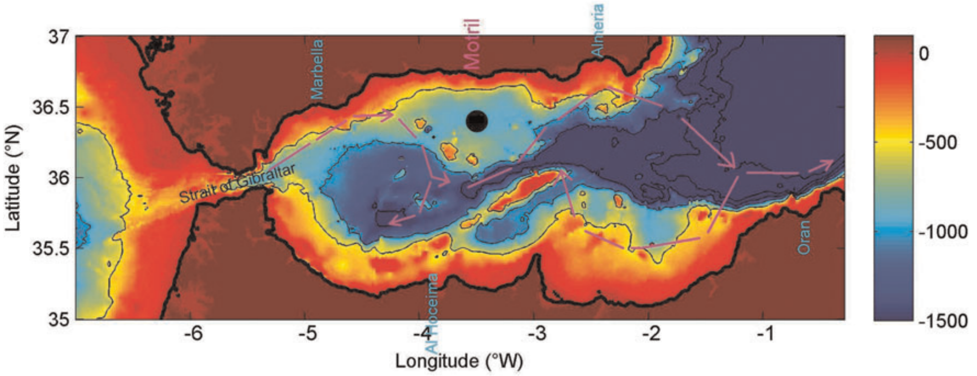

Fig. 1. Mooring test site (black dot) in the Alboran Sea. Black water-depth contours are drawn every 500 m; the thick-black contour indicates the 0-m coastline. The general Atlantic inflow frontal border is indicated by purple line arrows (after L'Helguen *et al.*, 2002).

The nearby Strait of Gibraltar separates relatively fresh and cool Atlantic Ocean waters from saltier and warmer Mediterranean waters. It is also a known source for 'solitary' high-frequency internal wave generation (Armi and Farmer, 1985; Watson and Robinson, 1990; Richez, 1994). This is because of the strong tidal currents, having amplitudes of up to 1.5 m s^{-1}, flowing back and forth over the relatively shallow Camarinal Sill of ~250 m. These highly nonlinear waves may transport suspended material including phytoplankton (Bartual *et al.*, 2011). They radiate into the Alboran Sea, but are not observed eastward of the line Marbella-Al Hoceima (Fig. 1; Watson and Robinson, 1990). This is approximately the border of southward deflection of Atlantic inflow near the surface, topographically steered by relatively shallow sills to its West around 4°W, before turning northeastward again towards Almeria (Fig. 1, e.g. L'Helguen *et al.*, 2002; Skliris and Beckers, 2009; Navarro *et al.*, 2011).

The Alboran Sea is thus a highly productive region of the Mediterranean (Champalbert, 1996). High productivity is found in the Atlantic inflow, as established in the upper 200 m for zooplankton (Thibault *et al.*, 1994) and near-surface phytoplankton (Navarro *et al.*, 2011). This inflow creates fronts with the surrounding Mediterranean waters. A well-known, high production area is the Almeria-Oran front, 100–200 km east of the present mooring site. Thus, the present test site is little affected by Atlantic inflow and mainly immersed in Mediterranean waters. This central-northern part of the Alboran Sea, northeast of the 4°W sills, is a relatively quiescent, topographically featureless basin, with different physics compared with the Strait of Gibraltar (Macias *et al.*, 2010). For example, tidal and residual current amplitudes are a tenth of those of the Strait of Gibraltar; high-frequency internal wave breaking and mixing processes are much less vigorous. Different physics naturally has effects of bio-physical coupling. For example, zooplankton species show a scattered DVM behaviour in the Strait of Gibraltar, whereas a clear sunset ascent and sunrise descent are observed in the Mediterranean water masses of the Alboran Sea (Frassetto *et al.*, 1961).

A comprehensive study on zooplankton abundance and taxonomy down to 700 m has been made by Andersen *et al.* (Andersen *et al.*, 2004), who also studied the Mediterranean water side of the Almeria-Oran front using multiple net sampling in wintertime. Associated acoustic sampling (Fielding *et al.*, 2001) showed a large scattering layer around 400 m, which was attributed to *Cyclothone* fish which did not undergo DVM. A fish species that did show DVM, *Bentosema glaciale*, migrated between 200 and 400 m, but it contributed only 0.4% to the total macroplankton (Andersen *et al.*, 2004). These authors reported that the most abundant species showing DVM in Mediterranean waters were copepods *Eucalanus monachus*, *Pleuromamma abdominalis*, *Pleuromamma borealis* and macroplankton *Euphausia krohni*, *Nematoscelis megalops*. All showed DVM between ~100 and 300 m, although the copepods demonstrated a preference for deeper waters when they were larger and in later life stages (mainly adult). Large *Nematoscelis megalops* were found to migrate between about 300 and 600 m, although uncertainties were considerable. To these species, one can add the occurrence of sufficiently large (>0.01 m) amphipods *Brachyscelus crusculum*, *Platyscelus ovoides*, *Streetsia challengeri* and the euphasiid *Thysanopoda aequalis* (Madin, 1991; for the Alboran Sea partially based on data of Rodríguez *et al.*, 1982).

All species are detectable by a 75 kHz acoustic system, which is sensitive to suspended particles and organisms larger than 0.005–0.015 m (Frassetto *et al.*, 1961; RDI, 1996; Mutlu, 2006), which include, besides fish, stage V and adult copepods (Madin, 1991).

METHOD

A taut-wire mooring was deployed at 36°24′N, 3°30′W, 912 m water depth between 2 and 11 April 2013. The area is more or less the deepest part of the central-north Alboran Sea, flat bottomed for several 10s of kilometres around, and about 40 km south of the harbour of Motril (E), facing the Sierra Nevada.

A single elliptic floatation provided 3000 N of net buoyancy at about 100 m from the bottom. With currents of typically less than 0.15 m s^{-1}, the buoy did not move more than 0.1 m vertically and 1 m horizontally, as was verified using pressure and tilt sensors. The float held an upward looking 75 kHz, four-beam Teledyne-RDI Longranger Acoustic Doppler Current Profiler (ADCP) that sampled at a rate of once per minute. The ADCP ranged 600 m, up to 180 m from the surface, in 10 m vertical bins. At such a range, the current components [u, v, w] (East, North, up) are averaged over several 100s of meters horizontally due to an acoustic beam slant of 20° to the vertical. The 'redundant' fourth beam provides the opportunity of calculating an 'error velocity' e, which is best considered as a white-noise estimate for w. In contrast, the echo-amplitude $I_j(z)$ [dB] is measured within the individual (1° spread) beams $j = 1, \ldots, 4$. At given depth, measured individual echoes are thus horizontally apart over the same several 100s of meters but average over <10 m. Here, we correct for sound attenuation in water as a function of range by subtracting the time mean at a particular depth, yielding the 'relative echo-amplitude' $dI(z) = I(z) - <I(z)>$ [dB], where the subscript is dropped and the $<>$ denotes averaging over the entire time series.

The lower 100 m of the vertical range, closest to the instrument, delivered some noisy data, which was assumed to be due to a lack of scatterers. However, visual inspection of the experimental mooring lines using video from the bottom to about 200 m from the surface showed turbid waters and lots of zooplankton throughout, see examples in Fig. 2. Unfortunately, species, sizes and thus (75 kHz) acoustic properties could not be determined from the video screening, so that we must assume that the noisy data are due to a decrease in acoustic back scattering with unknown cause.

Every other day, a conductivity–temperature–depth (CTD) profile was made from 5 m below the surface to 10 m above the bottom, at a horizontal distance of about 1 km from the mooring. A calibrated SeaBird 911plus CTD was used, sampling at 24 Hz, so that on average samples were obtained every 0.04 m.

RESULTS

Entire time series

The entire 9 days 600 m time-depth series of the (relative) acoustic echo-amplitude are characterized by a diurnal variation in amplitude, but in the upper half of the water column only (Fig. 3a). The diurnal variation is caused by the DVM of zooplankton, which has a typical vertical scale of 300 m and which can also be observed in the ADCP's vertical current (Fig. 3b). This vertical zooplankton motion, not representing vertical fluid particle motions, is best visible during the downward (blue) motion in the morning of every day. The typical daytime zooplankton resting depth is 350 m, with extension down to 500 m on the first day in the record (Fig. 3a).

The diurnal variation seems modulated by two signals of different periodicity. First, the deeper group migrating

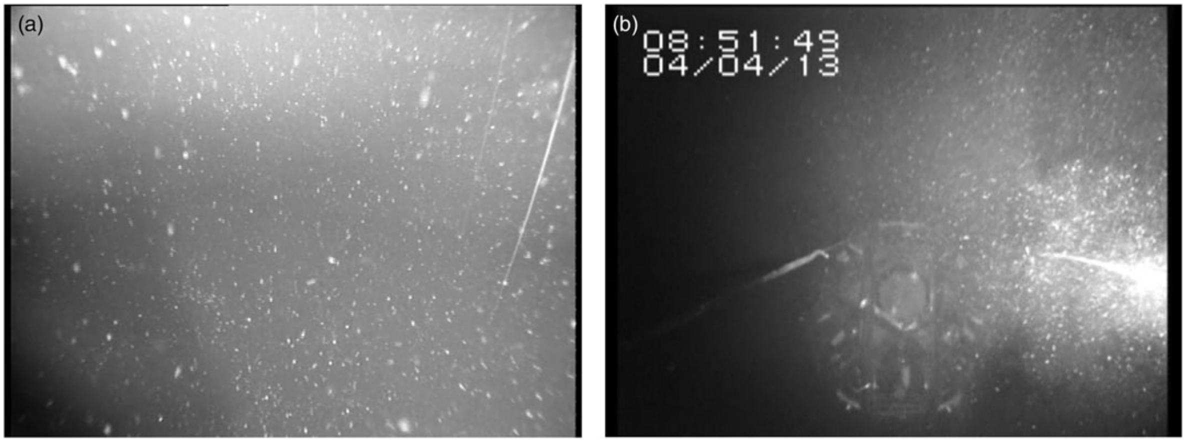

Fig. 2. Video stills from the experimental KM3NeT-mooring test, near the ADCP mooring. (**a**) Half-way up the experimental KM3NeT-mooring lines to the right, made from an ROV which was about 2 m horizontally away from the lines that are 0.4 m apart. (**b**) Looking upward from the bottom weight just after the launch of the self-unrolling mooring compacted in a 2-m-diameter aluminium sphere.

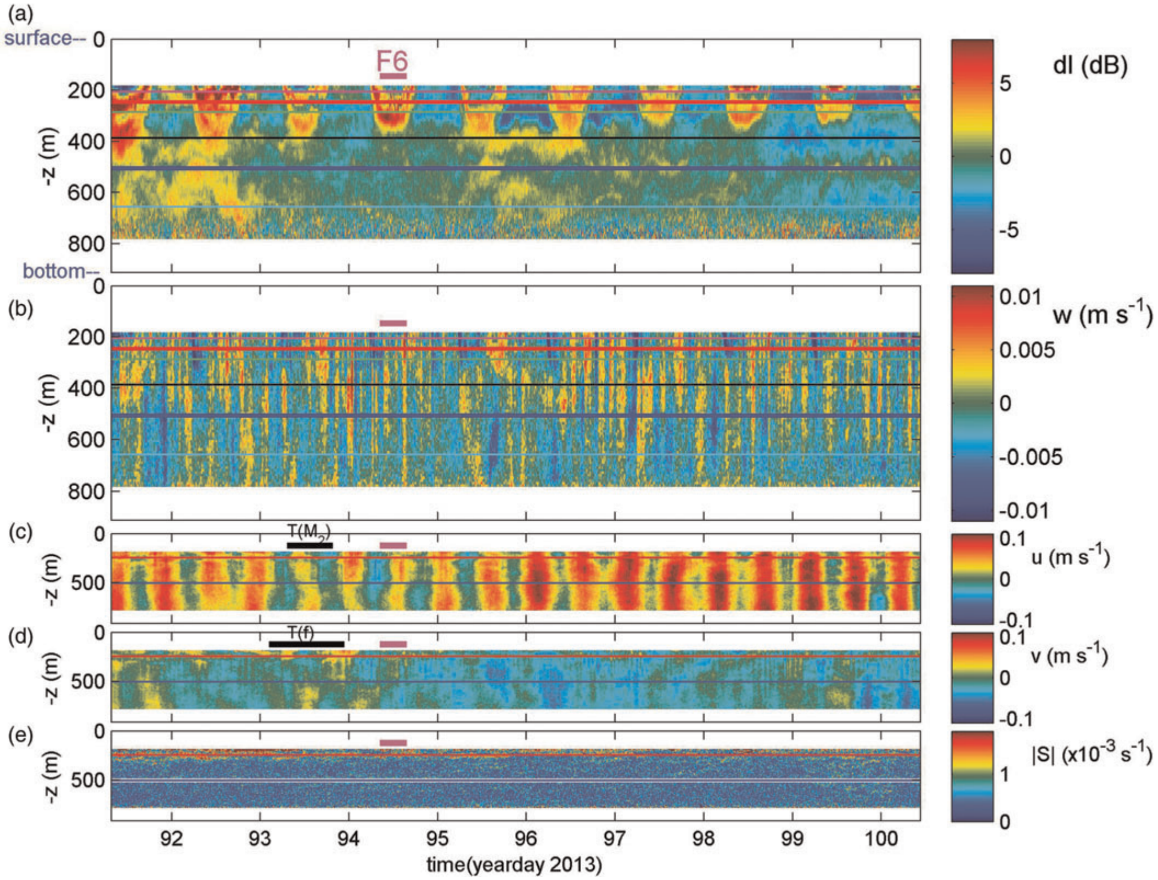

Fig. 3. Depth time images over the entire 600 m and 9 days ranges of 75 kHz ADCP data from the central-north Alboran Sea in April 2013. The six coloured horizontal lines indicate depth levels for which spectra are computed in Fig. 4. The horizontal purple bar indicates the short time range to be displayed in Fig. 6 'F6'. (**a**) Raw relative echo-amplitude. (**b**) Vertical current, smoothed over 20 min intervals to reduce noise. (**c**) East-west current, 20 min smoothed. Only red and blue lines repeated for clarity. (**d**) As c, but for north-south current. (**e**) As c, but for shear magnitude.

between about 300 and 500 m seems to vanish after 3 days in the record. This suggests a modulation by a long period motion >10 days, which could be the fortnightly spring-neap or the monthly lunar cycle. Although the precise modulation cannot be established from the 9-day record, it is noted that new moon was on 10 April 2013, when minimum migration was observed (day 99 in Fig. 3). Monthly lunar modulation of DVM has been observed in the deep ocean previously (van Haren, 2007). Second, around 250 m (the red line) high-frequency internal waves are observed (barely visible in Fig. 3; a zoom will be presented in Fig. 6 below), but only during daytime when (the upper group of) zooplankton was concentrated at depth levels just below. Such high-frequency waves were not observed every day, the most intense period being observed on day 94. At greater depths, the irregularly varying echo-amplitude occasionally showed, mainly low-frequency, internal wave modulation of up to 100 m crest-trough, especially around 500 m (blue line).

The blue line approximately divides the water column in more intense (high-frequent) vertical motions above and less intense, less frequent ones below (Fig. 3b). The vertical coherence length scale for high-frequency *w* can be the entire ADCP range (e.g. on day 94.6), but commonly it covers a shorter vertical range as the majority of high-frequency *w* are only found in the upper half of the ADCP range. This division is only vaguely observed in the generally vertically homogeneous along-channel horizontal current component *u* (Fig. 3c), and which is dominated by the semidiurnal tide. In contrast, the division is clearly seen in the weaker cross-channel horizontal current component *v* (Fig. 3d), which is dominated by the inertial motions that have a period of 20.2 h here. Especially around days 93–94, the checker board pattern in *v* indicates 180° phase difference, or maximum (large scale ≈ 100 m) shear, across the blue line at this depth. On the 10-m vertical scale however, shear barely exceeds the noise level around this depth (Fig. 3e).

A similar transition is found in v across the red line, which appears to indicate a minimum in u, or again, maximum shear. At that depth, in the upper 100 m of the range, the 10-m shear significantly exceeds the noise level, with values of up to about $2 \times 10^{-3}\ \mathrm{s}^{-1}$ (≈25 cpd, cycles per day) in a relatively thin layer and dominant at the inertial frequency f (Fig. 4d, below). This is common in well-stratified waters, in which the shortest vertical length scales are found at f (e.g. van Haren *et al*., 1999). Note that (1−2 m) thin layers are rather poorly resolved by the 10 m vertical bin size of the ADCP.

The above is confirmed in spectra for the entire period (Fig. 4), at the six depths of colour lines. The upper-range purple, red and green spectra of echo-amplitude (Fig. 4a) show clear peaks at (solar) diurnal and higher harmonics frequencies, showing DVM dominance. Largest variance is found at about 300 m (green), just below which the plankton concentrates during daytime. Below the black (400 m) level at which small diurnal (higher harmonic) peaks are observed, the absence of a diurnal peak for the deeper blue and light-blue levels confirms (virtually) no DVM.

At higher frequencies, the green, red and purple spectra show considerably more variance than the black, blue and light-blue spectra. This is unlikely to be associated with the enhanced buoyancy frequency at the higher levels (the one for the red level is indicated in Fig. 4). Although at 250 m (red), N is about twice the value at 400 m (black), see the CTD data in Fig. 5, there is no *a priori* reason why this would affect the plankton motions.

Gyroscopic convection

While at 400 m (black), the echo-amplitude spectrum (Fig. 4a) still weakly peaks at the diurnal frequency, the blue spectrum from 500 m peaks at an unusual intermediate frequency $\sigma = f/2 + f_h/2$ precisely between the frequencies of the vertical (f) and horizontal (f_h) Coriolis parameters. The latter becomes important for internal wave motions and convection in weakly stratified waters

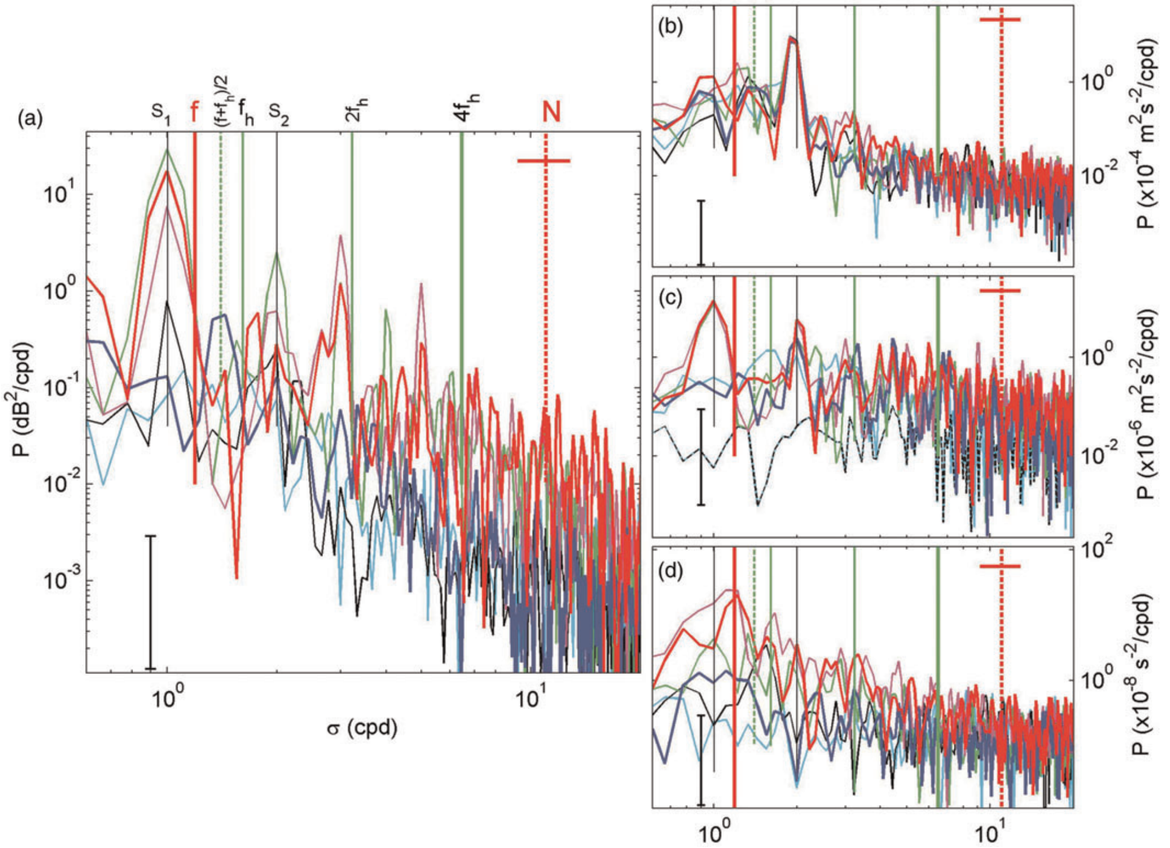

Fig. 4. Nearly raw (5 degrees of freedom) spectra at the depths indicated by the colour lines in Fig. 3. The indicated buoyancy frequency is computed from CTD data (Fig. 5) for the red (250 m) depth level. The vertical bar indicates the 95% significance level, valid for non-harmonic white noise signals. Focus is on the internal wave band, roughly for frequencies in the range [f, N], and on the frequencies related with DVM (S_1 and its higher harmonics). (**a**) Relative echo-amplitude from beam 1, dI_1. (**b**) Kinetic energy. (**c**) Vertical current. The black (400 m) spectrum is replaced by the light-blue-black-dashed line for the e(white noise)-spectrum at 650 m. (**d**) Shear (note change in vertical-scale range).

where buoyancy frequency $N = O(f)$ (LeBlond and Mysak, 1978; for a review see Gerkema *et al.*, 2008). This is because for very weak stratification, the gravitational vector no longer dominates as a restoring force, and convection of water being transported up and down in narrow 'tubes' moves towards the direction of the earth rotational vector (Straneo *et al.*, 2002; Sheremet, 2004). No forcing is known at $\sigma = f/2 + f_h/2$ and it may either reflect interaction between motions at $\sigma = f$ and $\sigma = f_h$ or a gradual increase of the local inertial frequency with depth, requiring mesoscale eddy-vorticity of up to $0.2f$. Both the *u*- and *v*-spectra, and thus the kinetic energy spectrum (Fig. 4b), also (sub-)peak at this intermediate frequency at the same depth, while at shallower depths (where the stratification is larger), the peak shifts to the local f (purple). The *w*-spectrum (Fig. 4c) shows diurnal (higher harmonic) peaks related to DVM for the upper three levels, but a peak at $\sigma = f_h$ for the light-blue (650 m) level. This peak seems insignificant compared with the rest of the *w*-spectrum, but it is better compared with the true white noise in *e* (dashed light-blue-black); *w* exceeds *e* for $\sigma < N$. At 650 m, the shear spectrum (Fig. 4d) is basically white noise. At shallower depths however, it indeed peaks at f [weakly for the blue (500 m) level, strongly for the red, purple (250, 200 m) levels]. In between, for the black (400 m) level, it peaks at a frequency close to f_h.

The variation in (internal wave) environment is reflected in the vertical density stratification. Nearby CTD observations do show a strong decrease in stratification with depth, by a factor of 4 between 270 and 380 m (that is a factor of 2 in N in Fig. 5a). Below about 400 m, there seems to be a slower decrease in N with depth or even a blocking at $N = 4f_h$ (below 550 m), definitely at $2f_h$ (below 700 m). These two specific buoyancy frequencies designate particular stability in stratification, usually in thin layers, that precisely balances shear by convective motions in the direction of the earth rotational vector (van Haren, 2008). These observations suggest relatively strong vertical (near-inertial) currents with amplitudes of 0.005–0.01 m s^{-1} that are persistent for several (up to 8) hours up or down, so that any suspended material is displaced by 100–200 m vertically. This results in *w*-spectra showing most variance in the f–f_h band below 500 m and peaking around 650 m. In addition to the near-inertial ('slantwise') convection in the direction of the earth-rotational vector at these depths, the 9-day mean vertical current amounts $< -1 \times 10^{-3}$ m s^{-1}, or a downward velocity of about 100 m day^{-1} (Fig. 5b). These vertical velocities and excursions are comparable to typical values observed for zooplankton DVM, of 0.01–0.05 m s^{-1}, but lasting only for 1.5–2 h, and 300 m, respectively (e.g. Frassetto *et al.*, 1961; Plueddemann and Pinkel, 1989).

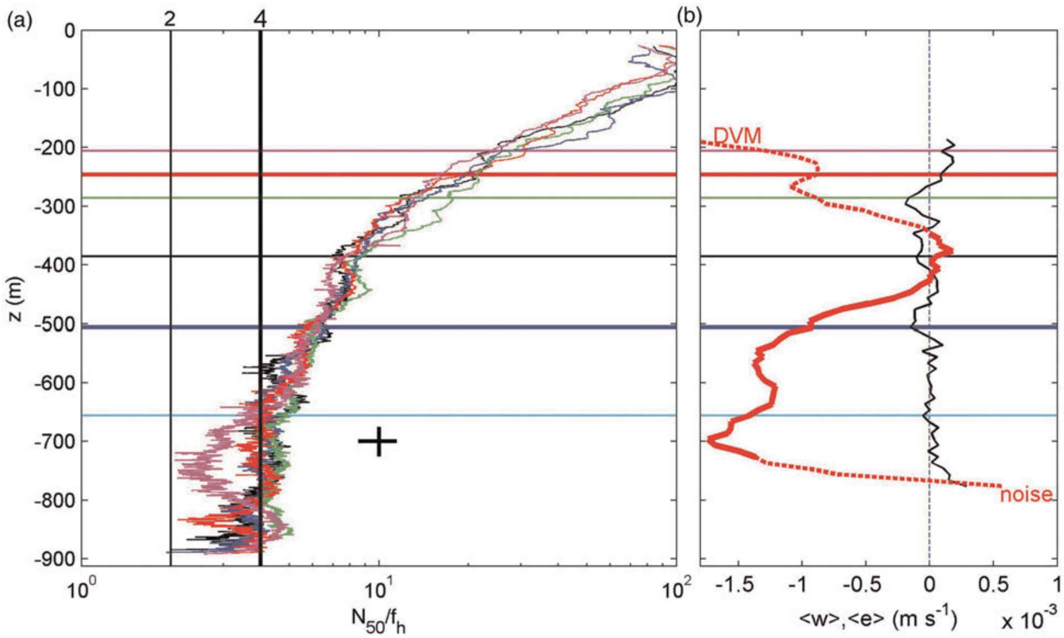

Fig. 5. Vertical profiles on stratification and time-averaged vertical velocity. (**a**) Buoyancy frequency ($\Delta z = 50$ m) scaled with horizontal Coriolis parameter (f_h) and computed for five different CTD profiles near the ADCP mooring. The cross indicates the approximate ± standard deviation in N-computation. The six horizontal colour lines indicate depth levels of ADCP data (Fig. 3). (**b**) Nine-day average vertical velocity (thick red) and error velocity (thin black). The dashed portions in the *w*-profile indicate depths where DVM or low-scatter noise dominate the signal, resulting in a bias of the estimate on water motion.

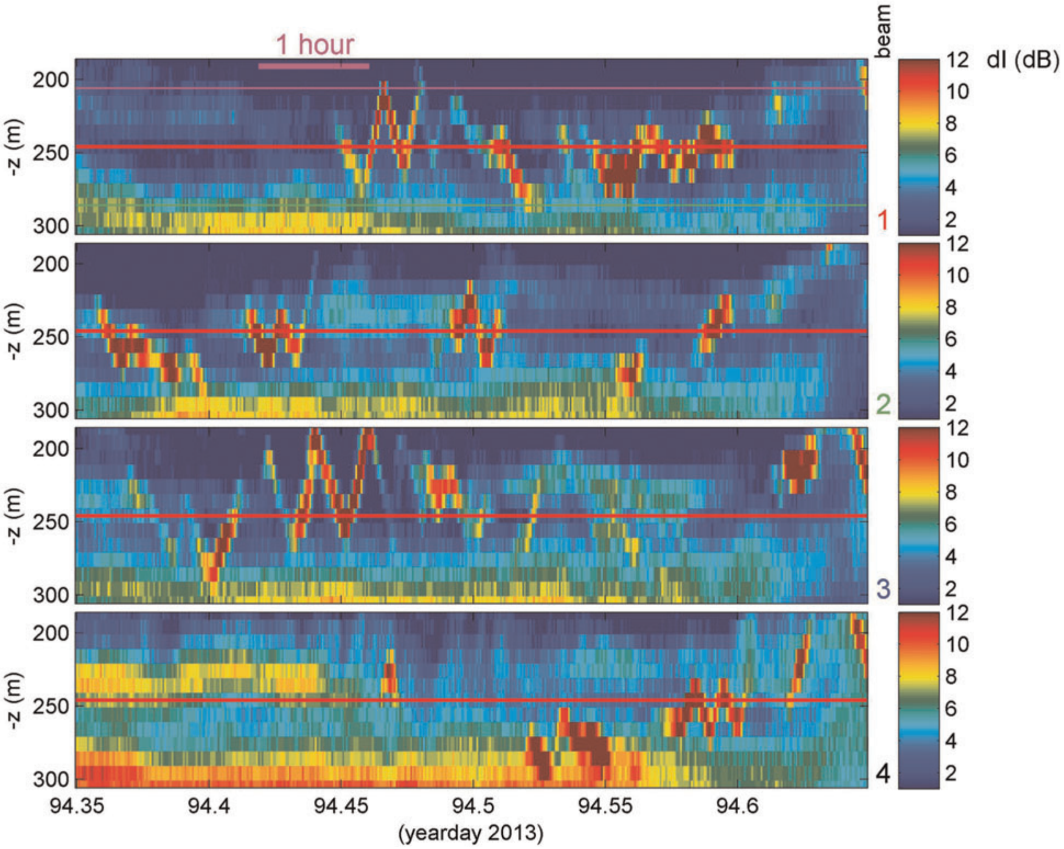

Fig. 6. Particular detail time-depth series of relative echo intensity for all four beams focusing on the top 100 m of the ADCP range where night-time-near-surface-zooplankton stay around mid-day. Note the shifted colour bar with respect to Fig. 3a; in the intense internal wave layers d*I* values go up to 18 dB (here given by saturated red colour for display purposes). The 3(1) horizontal colour lines in the panels for beams 1(2–4) are identical to those in Fig. 3.

For zooplankton, such near-inertial vertical currents would imply a considerable displacement in addition to their DVM. As the large vertical excursions are also imposed on the slightly stronger stratified layers above, see around the blue line in Fig. 3b, one could wonder whether the plankton deliberately avoids such con(-/ad) vective motions.

High-frequency internal waves concentration

Of smaller amplitude, but still covering several 10s of (up to 90) m crest-trough, are high-frequency internal waves that are particularly observed around 250 m, just above the depth where zooplankton is concentrated during daytime (Fig. 6). This is not the depth where strongest stratification is observed, cf. Fig. 5 which shows maximum N at 100 m or shallower. The observed period of slightly larger than half an hour for the large-amplitude waves corresponds well with the buoyancy frequency of some 30–40 cpd. Triangular shape, rather than sinusoidal shape as is common for linear waves, high-frequency internal waves have been observed in other areas, e.g. in the open NE-Atlantic Ocean using high-resolution temperature sensors (van Haren and Gostiaux, 2009). There, these waves moved (a few m) thin layers up and down, and, despite their triangular shape, did not show turbulent overturning exceeding the 2.5 m separation distance between the 52 sensors. The typical amplitudes of the waves were several 10s of meters (10–40 m crest-trough). It is noted that the ADCP was mounted in a free-spinning buoy, which rotated by about 50° and back between days 94.4 and 94.65. This somewhat hampers a directional analysis of the waves between the observations of echo-amplitude in all four beams, which are spread by some 300 m horizontally at this distance from the instrument. The large waves around day 94.45 seem to come from the south, as they are observed in beams 3 and 1 while the instruments' heading slowly moved from SSW to SSE, and back. The lack of the waves' registration in beams 2 and 4 suggests a wavelength shorter than 300 m, which is common for near-buoyancy frequency internal waves. This adds to the erratic behaviour in the wave pattern of Fig. 6. Speculating on a possible source, these high-frequency internal waves may result from large-scale internal wave interaction between near-inertial waves and the front to the south, or, more likely, following interaction with the topographic sills to the south of the mooring site (Fig. 1). It is noted that in such a case, they should not dissipate within about 30 km, or say 100 wavelengths. For comparison, this is roughly half the distance travelled by internal solitary waves generated in the Strait of Gibraltar and which dissipate in the western basin of the Alboran Sea (Watson and Robinson, 1990).

The images in Fig. 6 have a colour scheme for echo-amplitude values that are 8 dB higher than in Fig. 3a. Interfacial (thin layer) non-turbulent internal waves cannot account for such an increase in (75 kHz) acoustic response, as is shown here in the lack of such a response at other depths. It thus seems that it reflects enhanced abundance of zooplankton gathered on the waves. In contrast with other findings, mainly on phytoplankton (e.g. Franks, 1995), the zooplankton concentration is just not in internal wave troughs but seems uniform over the entire wave. The enhancement of acoustic reflective properties by the concentration of the zooplankton not only makes these high-frequency internal waves visible at this particular depth. It also shows that the zooplankton may be using the internal waves as feeding grounds on the plentiful phytoplankton during an unintentional and, perhaps, predator-risky free ride. The internal waves appear only fragmentary in Fig. 6. In part, this associates with the intermittent character of internal waves appearing in groups of a few waves. Here, it will partially be associated with the dispersal of zooplankton aggregations.

The considerably improved internal-wave-detection increase by the zooplankton behaviour is also seen in the high-frequency part of the acoustic echo spectra (Fig. 7), which show not only peaks at 48 cpd (half hour periodic motions), but also at higher frequencies (due to smaller amplitude internal waves). One would perhaps classify the vertical current spectrum (an average over the horizontal beam spread of all four beams) as somewhat erratic in the $\sigma = 10-100$ cpd band. The waves do not appear in the four beams simultaneously. Throughout this frequency band, the dI are elevated in most beams, certainly above noise level, but also above levels from depths where such internal waves were not observed, see the thin-red-dashed reference example from 600 m. The additional echo-amplitude information demonstrates that the interfacial waves are realistic and significant, also in the w-spectrum (purple), in which several peaks exceed the flat white noise level.

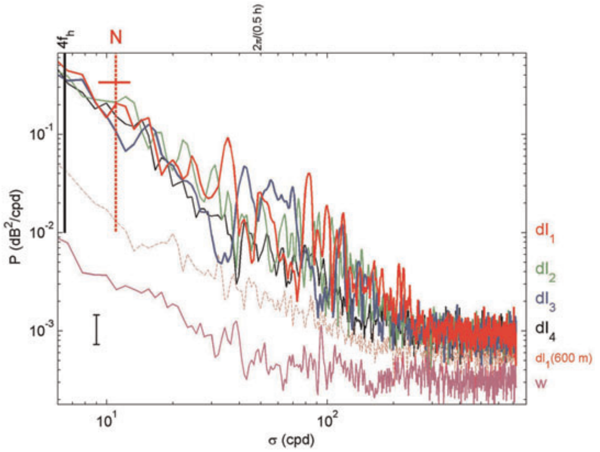

Fig. 7. Moderately smoothed spectra from entire time series at 245 m (the red line in Fig. 3) for all four beams $j = 1, \ldots, 4$ relative echo intensity dI_j and beam-averaged vertical current (arbitrarily off-set in the vertical). For reference, the dI_1 spectrum from 600 m is also given (thin-red dashed).

DISCUSSION AND CONCLUSIONS

The present observations suggest a feedback mechanism between physical water motions by internal waves and zooplankton behaviour.

On the one hand, zooplankton use the environmental variability of high-frequency internal waves for feeding, at the risk of being predated when the internal wave crests come too high up (it is noted that due to the relatively turbid waters little sunlight will penetrate down to 200 m, thereby hampering visual predation). In return, the high-frequency internal waves are only observed (in acoustic echo-amplitude) just above depths where zooplankton gather, and not at other depths. This contrasts with previous findings from mainly near-surface observations (e.g. Huber *et al.*, 2011). One could argue that the triangular patterns are unlikely to reflect vertical paths of zooplankton (or fish): there is no particular reason why they would move more or less precisely at the buoyancy frequency.

On the other hand, zooplankton are observed to limit their DVM to depths where stratification is relatively strong. It is unlikely that the zooplankton avoid the dark waters deeper than 500 m simply because of relative darkness, as open-ocean observations show DVM at depths >1000 m, although far from the bottom (>2000 m) (e.g. Vinogradov, 1961; Plueddemann and Pinkel, 1989; van Haren, 2007). At such depths not a single sunlight photon can penetrate (Kampa, 1970). There in the ocean, stratification was considerably larger than in the lower half of the Alboran Sea observed here. As a result, there must be a different reason for the lack of DVM at depths greater than 500 m in the Alboran Sea.

At these depths, stratification was so weak that relatively large, rather persistent vertical motions, mainly downdraught, were observed. The plankton seemed to limit their DVM to avoid such downdraughts or they became dispersed to deeper waters. Whether or not this is plankton-species-dependent is unknown, and this biophysical coupling requires further zooplankton research.

The present observations may not be limited to the central-north Alboran Sea. This is because, physically, the stratified central-north Alboran Sea acts like an open ocean, with stratification varying with depth supporting various internal waves. Fronts and meso-scale eddies are somewhat less important in this part of the Mediterranean. The observed deeper near-inertial convection in the weak stratification can be found in other parts of the Mediterranean, notably in those areas where deep dense-water convection is found, mainly in winter. Such convection is known to create relatively strong vertical motions and it will be interesting to see whether this hampers zooplankton DVM.

Biologically, differences in zooplankton DVM do exist between species. However, it is not expected that the observed interaction with internal waves is particular for the Mediterranean species that composed the present acoustic echoes. Although simultaneous net tows are lacking, DVM and internal wave interaction are such common features for many zooplankton species that the present observations are expected to occur elsewhere too, also outside the Mediterranean.

ACKNOWLEDGEMENTS

I thank captain and crew of the R/V Pelagia and NIOZ-MTM for deployment and recovery of the instrumentation.

FUNDING

This research has been funded in part by the Netherlands Organization for scientific research (NWO).

REFERENCES

Andersen, V., Devey, C., Gubanova, A. *et al.* (2004) Vertical distributions of zooplankton across the Almeria-Oran frontal zone (Mediterranean Sea). *J. Plankton Res.*, **26**, 275–293.

Armi, L. and Farmer, D. M. (1985) The internal hydraulics of the Strait of Gibraltar and associated sills and narrows. *Oceanol. Acta*, **8**, 37–46.

Bartual, A., Macias, D., Gutierrez-Rodriguez, A. *et al.* (2011) Transient pulses of primary production generated by undulatory processes in the western sector of the Strait of Gibraltar. *J. Mar. Syst.*, **87**, 25–36.

Champalbert, G. (1996) Characteristics of zooplankton standing stock and communities in the Western Mediterranean Sea: relations to hydrology. *Sci. Mar.*, **60** (Suppl. 2), 97–113.

Dekshenieks, M. M., Donaghay, P. L., Sullivan, J. M. *et al.* (2001) Temporal and spatial occurrence of thin phytoplankton layers in relation to physical processes. *Mar. Ecol. Prog. Ser.*, **223**, 61–71.

Durham, W. M. and Stocker, R. (2012) Thin phytoplankton layers: characteristics, mechanisms, and consequences. *Ann. Rev. Mar. Sci.*, **4**, 177–207.

Fielding, S., Crisp, N., Allen, J. T. *et al.* (2001) Meso-scale subduction at the Almeria-Oran front. II. Biophysical interactions. *J. Mar. Syst.*, **30**, 287–304.

Franks, P. J. S. (1995) Thin layers of phytoplankton: a model of formation by near-inertial wave shear. *Deep-Sea Res. I*, **42**, 75–91.

Frassetto, R., Backus, R. H. and Hays, E. (1961) Sound-scattering layers and their relation to thermal structure in the Strait of Gibraltar. *Deep-Sea Res.*, **9**, 69–72.

Gerkema, T., Zimmerman, J. T. F., Maas, L. R. M. *et al.* (2008) Geophysical and astrophysical fluid dynamics beyond the traditional approximation. *Rev. Geophys.*, **46**, RG2004, doi:10.1029/2006RG000220.

Huber, A. M. R., Peeters, F. and Lorke, A. (2011) Active and passive vertical motion of zooplankton in a lake. *Limnol. Oceanogr.*, **56**, 695–706.

Kampa, E. M. (1970) Underwater daylight and moonlight measurements in the eastern North Atlantic. *J. Mar. Biol. Assoc. UK*, **50**, 97–420.

LeBlond, P. H. and Mysak, L. A. (1978) *Waves in the Ocean*. Elsevier, Amsterdam NL, 602 pp.

Lennert-Cody, C. E. and Franks, P. J. S. (1999) Plankton patchiness in high-frequency internal waves. *Mar. Ecol. Prog. Ser.*, **186**, 59–66.

L'Helguen, S., Le Corre, P. and Madec, C. et al. (2002) New and regenerated production in the Almeria-Oran front area, eastern Alboran Sea. *Deep-Sea Res. I*, **49**, 83–99.

Linden, P. F. (1979) Mixing in stratified fluids. *Geophys. Astrophys. Fluid Dyn.*, **13**, 3–23.

Macias, D., Somavilla, R. and Gonzalez-Gordillo, J. I. et al. (2010) Physical control of zooplankton distribution at the Strait of Gibraltar during an episode of internal wave generation. *Mar. Ecol Prog. Ser.*, **408**, 79–95.

Madin, L. P. (1991) Distribution and taxonomy of zooplankton in the Alboran Sea and adjacent Western Mediterranean: a literature survey and field guide. Technical Report, Harbor Branch Oceanographic Inst. Inc., Fort Pierce, FL, 148 pp.

McManus, M. A., Alldredge, A. L., Barnard, A. H. *et al.* (2003) Characteristics, distribution and persistence of thin layers over a 48 hour period. *Mar. Ecol. Prog. Ser.*, **261**, 1–19.

Mutlu, E. (2006) Diel vertical migration of *Sagitta setosa* as inferred acoustically in the Black Sea. *Mar. Biol.*, **149**, 573–584.

Navarro, G., Vazquez, A., Macias, D. *et al.* (2011) Understanding the patterns of biological response to physical forcing in the Alboran Sea (western Mediterranean). *J. Geophys. Res.*, **38**, L23606, doi:10.1029/2011GL049708.

Plueddemann, A. J. and Pinkel, R. (1989) Characterization of the patterns of diel migration using a Doppler sonar. *Deep-Sea Res.*, **36**, 509–530.

Prairie, J. C., Sutherland, K. R., Nickols, K. J. *et al.* (2012) Biophysical interactions in the plankton: a cross-scale review. *Limnol. Oceanogr. Fluids Environ.*, **2**, 121–145.

RDI (1996) *A Practical Primer.* San Diego: Teledyne-RDI, San Diego, CA, 32 pp.

Richez, C. (1994) Airborne synthetic aperture radar tracking of internal waves in the Strait of Gibraltar. *Prog. Oceanogr.*, **33**, 93–159.

Rodríguez, J., García, A. and Rodriguez, V. (1982) Zooplanktonic communities of the divergence zone in the Northwestern Alboran Sea. *Mar. Ecol.*, **3**, 133–142.

Sheremet, V. A. (2004) Laboratory experiments with tilted convective plumes on a centrifuge: a finite angle between the buoyancy and the axis of rotation. *J. Fluid Mech.*, **506**, 217–244.

Skliris, N. and Beckers, J.-M. (2009) Modelling the Gibraltar Strait/Western Alboran Sea ecohydrodynamics. *Ocean Dyn.*, **59**, 489–508.

Stemmann, L., Prieur, L., Legendre, L. *et al.* (2008) Effects of frontal processes on marine aggregate dynamics and fluxes: an interannual study in a permanent geostrophic front (NW Mediterranean). *J. Mar. Syst.*, **70**, 1–20.

Straneo, F., Kawase, M. and Riser, S. C. (2002) Idealized models of slantwise convection in a baroclinic flow. *J. Phys. Oceanogr.*, **32**, 558–572.

Sverdrup, H. U. (1953) On conditions for the vernal blooming of phytoplankton. *J. Cons. Perm. Int. Explor. Mer*, **18**, 287–295.

Thibault, D., Gaudy, R. and Le Fevre, J. (1994) Zooplankton biomass, feeding and metabolism in a geostrophic frontal area (Almeria-Oran front, western Mediterranean). Significance to pelagic food webs. *J. Mar. Syst.*, **5**, 297–311.

van Haren, H. (2007) Monthly periodicity in acoustic reflections and vertical motions in the deep ocean. *Geophys. Res. Lett.*, **34**, L12603, doi:10.1029/2007GL029947.

van Haren, H. (2008) Abrupt transitions between gyroscopic and internal gravity waves: the mid-latitude case. *J. Fluid Mech.*, **598**, 67–80.

van Haren, H. and Gostiaux, L. (2009) High-resolution open-ocean temperature spectra. *J. Geophys. Res.*, **114**, C05005, doi:10.1029/2008JC004967.

van Haren, H., Maas, L., Zimmerman, J. T. F. *et al.* (1999) Strong inertial currents and marginal internal wave stability in the central North Sea. *Geophys. Res. Lett.*, **26**, 2993–2996.

van Haren, H., Mills, D. K. and Wetsteyn, L. P. M. J. (1998) Detailed observations of the phytoplankton spring bloom in the stratifying central North Sea. *J. Mar. Res.*, **56**, 655–680.

Vinogradov, M. E. (1961) Feeding of the deep-sea zooplankton. *Rapp. P. V. Réun. Cons. Int. Explor. Mer.*, **153**, 114–120.

Warren, J. D., Stanton, T. K., Wiebe, P. H. *et al.* (2003) Inference of biological and physical parameters in an internal wave using multiple-frequency acoustic-scattering data. *ICES J. Mar. Sci.*, **60**, 1033–1046.

Watson, G. and Robinson, I. S. (1990) A study of internal wave propagation in the Strait of Gibraltar using shore-based marine radar images. *J. Phys. Oceanogr.*, **20**, 374–395.